Evaluation of an ozone diffusion process using a hollow fiber membrane contactor

Alice Schmitt, Julie Mendret, Stephan Brosillon

Evaluation of an ozone diffusion process using a hollow fiber membrane contactor

Alice Schmitt[a], Julie Mendret[a], Stephan Brosillon[a]

[a] IEM, University of Montpellier, CNRS, ENSCM, Montpellier, France

Submitted to Chemical Engineering Research and Design

Corresponding author:

Julie Mendret

IEM (Institut Européen des Membranes), UMR 5635 (CNRS-ENSCM-UM2),

Université Montpellier 2, place Eugène-Bataillon, F-34095 Montpellier, France

Tel: +33 467144624 ; Fax: +33 467149119

E-mail: julie.mendret@umontpellier.fr

Abstract

Conventional ozonation processes efficiently remove micropollutants in water treatment, but uncontrolled ozone dosing can produce problematic by-products. Bubbleless operation could help overcome this hurdle. To evaluate this alternative, ozonation was carried out using a polytetrafluoroethylene (PTFE) hollow fiber membrane contactor. The objective was to conduct an extensive characterization of the ozone transfer in an in/out configuration. The overall mass transfer coefficient K_La was determined and was higher than in bubble columns. The transfer resistance due to the membrane was estimated to be lower than 1%. The impact of several variables (liquid flowrate, gas flowrate, and ozone concentration) on the ozone transfer was studied. Ozone concentration was the variable that most increased ozone transfer, followed by the liquid flowrate and then to a lesser extent the gas flowrate. The impact of the presence of a reaction in the water was also evaluated using an organic dye (Acid Orange 7). The Hatta number and the acceleration factor were calculated, corresponding to a reaction that took place partially in the liquid film and in the liquid bulk. Finally, the impact of ozone on membrane material over time was evaluated.

Keywords: ozonation, hollow fibers, membrane contactor, mass transfer, Acid Orange 7

1. Introduction

Drinking water resources are precious and scarce. Their quality and quantities are decreasing significantly as the population rises. To preserve these resources and the water ecosystem, wastewater treatment plants (WWTPs) need to be upgraded by an advanced treatment to ensure the elimination of micropollutants, defined as harmful substances detectable in the environment at very low concentrations ($ng.L^{-1}$ to $\mu g.L^{-1}$). Wastewater treatment plants are one of the main sources of organic micropollutants released into the aquatic receiving environment. The micropollutants released by WWTPs are mostly active ingredients of pharmaceuticals (Bolong et al., 2009). Activated carbon adsorption and ozonation are two processes that can used to treat organic micropollutants in wastewater (Margot et al., 2013). The efficiency of activated carbon depends on dose of powdered activated carbon, regeneration of activated carbon granules, contact time, and the presence of natural organic matter, which can diminish micropollutant removal (Guillossou et al., 2020; Luo et al., 2014). Ozonation is effective and economic, easy to automate, and clean to handle. It offers a chemical way to remove 90% of emerging contaminants and can be simply incorporated into both existing and new applications (Prieto-Rodríguez et al., 2013; Snyder et al., 2006). During ozonation, a

Abbreviations: AO7: Acid Orange 7; DOE: design of experiments; PP: Polypropylene; PTFE: Polytetrafluoroethylene; PVDF: Polyvinylidene fluoride; SEM: Scanning Electron Microscopy

targeted substance is degraded by direct and indirect oxidation (unlike activated carbon, which only adsorbs). In addition, ozone is a disinfectant that can be used to inactivate some of the pathogens present in wastewater. Ozonation is thus a very appealing technology for water reuse, and it can be used coupled to other technologies in a multiple-barrier concept. However, ozone in water treatment is generally bubbled through diffusers. Bubbling has drawbacks, such as stripping of volatile organic compounds, high reactor footprints, mass transfer limitations (whence high energy costs) and foaming. Another disadvantage is the release, in some cases, of by-products of the oxidation reaction that may be more hazardous than the original pollutants (Gogoi et al., 2018; Schlüter-Vorberg et al., 2015). This concern often stems from uncontrolled ozone dosage. To overcome all these problems, the recent use of membrane contactors for ozone diffusion in water treatment offers an attractive solution, by virtue of its bubbleless operation (Schmitt et al., 2020). Membrane contactors have recently emerged as a good alternative to classic reactors for the transfer of gas to a liquid phase (Pabby and Sastre, 2013), and to control the dosing of ozone during ozonation processes by injecting it across the membrane through multiple dosing points (Merle et al., 2017). At neutral pH, ozone decomposition into hydroxyl radicals will allow the removal of a wider range of micropollutants. Simultaneously, the use of a membrane contactor for ozonation of water containing bromides may minimize the formation of bromates (regulated in drinking water because of their carcinogenic potential), through many ozone dosing points, leaving less residual ozone. Hence the use of this method for applications such as micropollutant treatment and bromate minimization appears very promising.

Membrane contactor technology for ozonation of water is not yet well described, and more work is needed to fully characterize the process. When ozone contactors are used, two configurations are possible. In one, the liquid flows inside the membrane, and the gas in the shell (i.e., outside the membrane). In the other, phases (liquid and gas) are reversed. Membranes can have various geometries: plane, tubular, capillary or hollow fiber. These last three forms are often used to transfer gas (e.g., ozone) to water, and differ in their pore diameter. Hollow fiber membranes have very small diameters (internal diameter < 0.5 mm), giving very large exchange surface areas per unit volume (Schmitt et al., 2020). To the best of the authors' knowledge, only one article to date reports on an experimental investigation of ozone transfer through a membrane contactor (tubular membrane) with the gas circulating inside the fibers and the liquid in the shell (i.e., in/out configuration) (Wenten et al., 2012). This configuration offers the main advantage of a lower risk of membrane fouling thanks to the circulation of the gas in the fibers whose the diameter is smaller than 1 mm instead of the

Abbreviations: AO7: Acid Orange 7; DOE: design of experiments; PP: Polypropylene; PTFE: Polytetrafluoroethylene; PVDF: Polyvinylidene fluoride; SEM: Scanning Electron Microscopy

treated wastewater which could have suspended matter. Wenten et al. had already shown that this configuration could produce a better oxidation of iodide into iodine, for instance. The authors suggested that the poorer result obtained with the out/in configuration could be due to a reaction between ozone and membrane ceramic material. It would thus be useful to confirm this observation and extend it, both for components other than iodide, and for other membranes such as polymer membranes, which are less costly and easier to use owing to their robustness. This was the objective of the present work.

Polymer hollow fiber membranes were used instead of the ceramic tubular membranes in Wenten et al. The overall goal of this work was to fully characterize the transfer of ozone from the gas phase to the liquid phase in an in/out hollow fiber membrane contactor. The aim was to determine (i) the impact of several operating variables (liquid flow rate, gas flow rate, ozone concentration in the gas mix), (ii) the process efficiency for the abatement of an organic dye (Acid Orange 7) as model solution, and (iii) the effect of the presence of ozone on membrane durability. This work thus contributes to a better understanding of the ozonation process for wastewater reuse using membrane contactors.

2. Materials and methods

2.1. Membrane contactor technology

The membrane contactor used in this work was supplied by Polymem (France). Its characteristics are listed in Table 1. Gas circulates inside the fibers and liquid in the shell by counter-current flow (Figure 1.b). The hollow fibers were made of polytetrafluoroethylene (PTFE), known to be highly ozone-resistant over time (Bamperng et al., 2010). The hollow fiber form enables a very compact process through a large exchange surface area.

Table 1. Membrane contactor technical specifications.

The membrane porosity ε ([a]) was determined gravimetrically (Sartorius CPA 225D balance), by measuring the mass of isopropanol (IPA) inside the membrane pores (Wang et al., 2010). The porosity was calculated as:

$$\varepsilon = \frac{(w_{\mathrm{wet}} - w_{\mathrm{dry}})/D_{\mathrm{iso}}}{\frac{w_{\mathrm{wet}} - w_{\mathrm{dry}}}{D_{\mathrm{iso}}} + w_{\mathrm{dry}}/D_{\mathrm{PTFE}}} \quad , [1]$$

where w_{wet} is the weight of the wet membrane, w_{dry} is the weight of the dry membrane, D_{iso} is the IPA density, and D_{PTFE} is the polymer density.

The tortuosity factor τ ([b]) was estimated by the porosity-tortuosity relationship defined by (Iversen et al., 1997) as:

$$\tau = \frac{(2-\varepsilon)^2}{\varepsilon} \text{ , [2]}$$

The liquid volume ([c]) and the specific exchange surface area ([d]) were calculated from the shell and fiber properties given by the manufacturer.

When using a membrane contactor, a very important variable to check is the transmembrane pressure. If the ratio of the pressure on the liquid side to the pressure on the gas side is higher than the "breakthrough pressure", wetting of the membrane pores occurs (i.e., the liquid penetrates the membrane pores), lowering the mass transfer. The breakthrough pressure (relative, in Pa) is defined by the Young-Laplace equation as:

$$P_{\text{breakthrough}} = \frac{4 \times \gamma \times \cos\theta}{d_{\text{pore,max}}} \text{ , [3]}$$

where γ is the surface tension of water with air (= 73 x 10^{-3} N.m^{-1} at 20 °C), θ is the contact angle between the membrane and the water (radians), and $d_{\text{pore,max}}$ is the maximum pore diameter (m) (determined from fiber SEM pictures analyzed with ImageJ® software)

In this work, the breakthrough pressure was estimated to be 0.4 bar (taking the contact angle between the material and the water to be greater than 102°).

Conversely, if the ratio of the pressure on the gas side to the pressure on the liquid side is higher than the "bubble pressure", there is ozone dispersion in water by bubbles. In this case, one of the main advantages of the membrane contactor, which is to transfer ozone uniformly to the water to be treated in a bubbleless operation, is lost. The bubble pressure was experimentally determined with the following method, adapted from the method presented by Khayet and Matsuura (Khayet and Matsuura, 2001). A special membrane contactor was produced for this test, with PTFE fibers provided by the same supplier (Polymem) as for the membrane contactor used in the experiments, but without a shell. Oxygen circulated inside the membrane fibers immersed in water. The oxygen pressure was then gently increased stepwise. The bubble pressure was considered attained when the first bubble was observable. With this method, the bubble pressure was estimated to be about 0.1 bar. Hence the transmembrane pressure (i.e., the difference between the pressure on the liquid side and the pressure on the gas side) had to stay between −0.1 and 0.4 bar.

To evaluate the hydrophobicity of the fibers before and after use, contact angle was measured using the sessile drop method with a GBX meter (Digidrop, France) equipped with image analysis software

(Visiodrop). First, fibers were fixed on a glass plate. A droplet of water (1 µL) was then deposited on the film surface with a precision syringe. The method is based on image processing and curve fitting for contact angle measurement from a theoretical meridian drop profile, determining two contact angles between the baseline of the drop and the tangents at the drop boundary (i.e., one angle is measured on the right and one on the left, the final contact angle being the average of the two values). Each measurement was repeated three times.

Scanning electron microscopy (SEM) pictures were obtained using a Hitachi S-4800 instrument to evaluate the state of the fibers and their deterioration after use. Samples were previously metalized with a thin layer of platinum to improve their electronic conductivity.

2.2. Ozonation: pilots and methods

- **Description of the ozonation pilot with membrane contactor – liquid in closed loop**

Figure 1.a depicts the experimental set-up used for the ozonation process. When the liquid was in a closed loop, this ozonation lab-scale pilot consisted of a membrane contactor (see Section 2.1 for description) continuously fed by an ozone generator (BMT 803 N) from a lab-grade pure oxygen tank. Before circulating in the gas side of the membrane contactor, the ozone was diluted with the oxygen to achieve the desired gas flowrate. An ozone gas analyzer (BMT 964) was used to monitor the gas ozone concentration ($C_{O3,gas,in}$) after dehumidification. Two electrovalves connected to a computer were used to determine the desired concentration of the oxygen/ozone mixture.

The liquid flowed into the pilot from a stirred 1.5 L glass tank under thermostatic control (20 °C). During the experiment, an agitator was used to homogenize dissolved ozone and dye concentrations in the tank. A peristaltic pump (Watson Marlow 323) was used for the liquid circulation. Two taps (upstream and downstream of the membrane contactor) were used for sampling.

Ozone was transferred from the gas phase of the membrane contactor to the liquid phase, along a concentration gradient. The membrane in the contactor acted as a barrier.

The main advantage of this configuration was to increase the residence time in the membrane contactor and has thus been used for the K_La determination (Section 3.1).

Figure 1. a. Flowsheet of the ozonation pilot - liquid in closed loop - gas in open circuit (red: gas stream, blue: liquid stream); b. Zoom on the configuration of the membrane contactor.

- **Description of the ozonation pilot with membrane contactor – liquid in open circuit**

The ozonation pilot with the liquid flowing in an open circuit was almost the same as in the closed loop. The main difference was that the liquid circulated only once in the membrane contactor. The liquid was then recovered in a container with KI solution to prevent the ozone degassing. To achieve the steady-state values, a larger feed tank was used (30 L). The tank was made of stainless steel, stirred, and under thermostatic control (20 °C). The main advantage of this configuration was the simplification of the mass balances in comparison to that with the liquid in closed loop. Therefore, this configuration has been used for the study of the impact of several variables on the ozone transfer and for the experiments with AO7 (Sections 3.3 and 3.4).

- **Description of the ozonation pilot with bubble column (batch reactor)**

To compare the results obtained with the membrane contactor with those obtained with a conventional process, a semi-batch bubble reactor was also used (see Figure 2). A 4 L glass reactor was stirred using an agitator to homogenize the liquid and kept under thermostatic control (20 °C). A recirculating pump was used for sampling. As in the previously described ozonation pilot with the membrane contactor, an oxygen cylinder fed the gas circuit. A gas flowmeter was then used to regulate gas flowrate upstream of an ozone generator (BMT 803 N). The ozone generator was used to convert part of the pure oxygen into ozone. The amount of ozone produced by the generator could be manually regulated with a setting knob. The gas mixture obtained therefore comprised ozone and oxygen. An electrovalve connected to a computer was used to set the gas flowrate and obtain the desired concentration of the gas mixture. Two options were then possible. The first was for the gas mixture to flow through the by-pass and be analyzed with an ozone analyzer (BMT 964) and then processed in an ozone destructor, in the same way as with the ozonation pilot with the membrane contactor. The ozone concentration given by the analyzer was then the ozone concentration in the gas at the inlet to the process. The other option was for the gas mixture to flow inside the semi-batch reactor with a porous diffuser, and then be analyzed and deozonated. The ozone concentration given by the analyzer was then the ozone concentration in the gas at the outlet from the bubble column. The analyzer was preceded by a dehumidifier to remove any humidity in the gas and protect the device. The residual ozone was destroyed by the ozone destructor using active carbon.

Figure 2. Scheme of the ozonation pilot with bubble column.

- **Design of experiments: determination and interpretation**

The analysis of the experimental data obtained with a 2^3 factorial design of experiments (DOE) was conducted to compare the significance and the impact of three variables on the ozone transfer, namely the liquid flow rate (Q_{liq}), the gas flow rate (Q_{gas}), and the ozone concentration at the gas inlet (C_{O3}). For each variable, three levels were tested (a minimum, a central point, and a maximum). Variables and their minima and maxima were chosen after a preliminary study of the literature, and were adapted to the capacity of the experimental pilot used (Schmitt et al., 2020). Minitab 19® software was used to establish and interpret the DOE.

- **Ozone analysis**

The indigo method (Bader and Hoigné, 1982) was used to determine the dissolved ozone concentration in the liquid phase. Once the experiment had started, the ozone gas analyzer (BMT 964) was used to analyze the gas ozone concentration at the outlet from the membrane contactor ($C_{O3,gas,out}$) (after dehumidification).

- **Inhibition of hydroxyl radicals**

During the ozonation reaction, several mechanisms act in parallel. Dissolved ozone can both react directly with the pollutant, or indirectly due to its decomposition into hydroxyl radicals (Roustan, 2003; Schmitt et al., 2020). The different matrices used in this work were buffered at acid pH (pH ≈ 3) to limit ozone decomposition (i.e., decomposition of molecular ozone into hydroxyl radicals), and therefore facilitate understanding of the ozone transfer. The buffered solution used was made by dissolving 1.2 $g.L^{-1}$ of sodium dihydrogen phosphate (NaH_2PO_4) in deionized water and then adjusting the pH with a few milliliters of 84% phosphoric acid (H_3PO_4). The pH of the final buffered solution was 2.2.

2.3. **Matrix characterization**

- Buffered water

Buffered water was made by mixing demineralized water (total organic carbon < 30 ppb) and the buffered solution described in the section “Inhibition of the hydroxyl radicals” to adjust the pH. The final pH of the matrix was 3.

- Solution colored with Acid Orange 7 (AO7)

Acid Orange 7 (AO7) ($C_{16}H_{11}N_2NaO_4S$, purity > 85 %), also called Orange II, was obtained from Sigma and used without further purification. AO7 was chosen as a model for organic pollutants owing to its high reactivity with molecular ozone and ease of analysis. AO7 concentration was measured in a 1 cm

plastic cuvette using a UV-VIS spectrophotometer (UV-2401PC, Shimadzu, Japan) at wavelength 484 nm (at which the absorption of AO7 is maximum).

2.4. Theoretical approach to ozone mass transfer in a membrane contactor

Figure 3 depicts the mass transfer in a gas-liquid membrane contactor. The membrane is hydrophobic, and so membrane pores are filled by the gas (i.e., non-wetted). The compound of interest (i.e., the ozone) encounters three flow resistances in series going from the bulk of the gas phase to the bulk of the liquid phase: the gas film (the gas-membrane boundary layer), the membrane, and the liquid film (the membrane-liquid boundary layer). At the interface between gas and liquid, the concentration profile is discontinuous and obeys Henry's law (Gabelman and Hwang, 1999).

Figure 3. Ozone concentration profile in a membrane contactor (adapted from Schmitt et al., 2020).

The overall mass transfer resistance, relative to the liquid side, is the sum of the individual mass transfer resistance in each phase and can be defined as $R_{ov} = 1/K_L$. For a membrane contactor where the liquid flows in the shell (i.e., outside the membrane) and the gas flows inside the fibers, it can be described as (Kukuzaki et al., 2010):

$$\frac{1}{K_{\mathrm{L}} \times A_{\mathrm{outer}}} = \frac{1}{H \times k_{\mathrm{g}} \times A_{\mathrm{lm}}} + \frac{1}{H \times k_{\mathrm{m}} \times A_{\mathrm{lm}}} + \frac{1}{k_l \times A_{\mathrm{outer}}}, \quad [4]$$

where K_L is the overall mass transfer coefficient (m.s^{-1}), k_m, k_g, k_l are the mass transfer coefficient in the membrane, in the gas, and in the liquid respectively (m.s^{-1}), A_{outer}, A_{lm}, A_{inner} are the outer, logarithmic mean, and inner surface area of the membrane respectively (m^2), H is the solubility (here of ozone) in water (dimensionless), which can be described by Henry's law as $H = (C_{O3,g}/C_{O3,l})$eq: for the dissolution of ozone in water, its value is 3.823 (mg/L)/(mg/L) at 295 K (Atchariyawut et al., 2009) and is reduced to 2.907 at 295 degrees Kelvin (Roustan, 2003).

After simplification of Equation 4, the global mass transfer coefficient can be expressed as:

$$\frac{1}{K_{\mathrm{L}}} = \frac{d_{\mathrm{o}}}{H \times k_{\mathrm{g}} \times d_{\mathrm{i}}} + \frac{d_{\mathrm{o}}}{H \times k_{\mathrm{m}} \times d_{\mathrm{lm}}} + \frac{1}{k_l^r}, \quad [5]$$

where d_i, d_{lm}, d_o are respectively the inside, logarithmic mean, and outside diameters of the fibers (m).

In Equation 5, describing the overall mass transfer from the resistance-in-series model, when a chemical reaction occurs, k_l can be replaced by $k_{\mathrm{l}}^{\mathrm{r}}$, defined as $k_{\mathrm{l}}^{\mathrm{r}} = E k_{\mathrm{L}}$. E is the enhancement factor, described by $E = \frac{J_{\mathrm{O_3\ with\ reaction}}}{J_{\mathrm{O_3\ without\ reaction}}}$. It takes into account the effect of the reaction on the mass

transfer, increasing by the rise in the concentration gradient (Nguyen, 2018). The resistance on the liquid side is therefore reduced by the presence of a chemical reaction in the liquid.

The membrane mass coefficient can be calculated from the membrane structure properties (Bamperng et al., 2010; Mavroudi et al., 2006) as:

$$k_{\mathrm{m}} = \frac{D_{\mathrm{O3,m}} \times \varepsilon}{\tau \times l_{\mathrm{m}}}, \text{ [6]}$$

where $D_{O3,m}$ is the effective diffusion coefficient of ozone in the membrane ($m^2.s^{-1}$) and l_m the membrane thickness (m). Inside the membrane pores, gas can flow by molecular diffusion and Knudsen diffusion. $D_{O3,m}$ can therefore be expressed as Equation 7 (Jansen et al., 2005).

$$D_{\mathrm{O3,m}} = \frac{1}{\frac{1}{D_{\mathrm{O_3,g}}} + \frac{1}{D_{\mathrm{K}}}} = \frac{1}{\frac{1}{D_{\mathrm{O_3,g}}} + \frac{1}{\frac{d_{\mathrm{pore}}}{3}\sqrt{\frac{8RT}{\pi M}}}}, \text{ [7]}$$

where D_K is the Knudsen diffusion coefficient, defined by $D_{\mathrm{K}} = \frac{d_{\mathrm{m,pore}}}{3}\sqrt{\frac{8RT}{\pi M}}$ ($m^2.s^{-1}$), $D_{O3,g}$ is the diffusion coefficient of ozone in the gas phase ($m^2.s^{-1}$) (= 2.00×10^{-5} $m^2.s^{-1}$ at 20 °C (Bamperng et al., 2010)), T is the temperature (293.15 degrees Kelvin), M is the molar mass of ozone (47.998 $g.mol^{-1}$, R is the ideal gas constant (8.3145 $J.K^{-1}.mol^{-1}$, and $d_{m,pore}$ is the mean pore diameter (m) (0.777 µm for the membrane contactor used).

This last value (the average membrane pore size) was determined by liquid-gas displacement porometry, using a PMR-2000-LL-R porometer (IFTS-France). The pores of the sample were filled with IPA during a first wetting step. Nitrogen gas was then fed through the membrane and its flowrate was measured as a function of the applied pressure. Pore dimension was next calculated by applying Laplace's law, which is expressed in Equation 8.

$$\Delta P = \frac{4\gamma \cos\theta}{d_{\mathrm{pore}}}, \text{ [8]}$$

where γ is the interfacial tension of IPA, ΔP is the differential of applied pressure, θ is the contact angle between the membrane and the IPA, and d_{pore} is the pore diameter.

3. Results and discussion

3.1. Determination of the global transfer coefficient $K_L a$

The overall material balance was first established. The conditions of liquid flow strongly impact the liquid transfer coefficient, and thereby the value of $K_L a$, which represents a sum of the different coefficients. Determining $K_L a$ is thus essential to compare several reactors. Turbulent flow of gas and

liquid phases makes the description of the velocity fields very complicated, and so overall coefficients are indispensable for the mass balance equation. In addition, the modeling of the ozone transfer through a membrane contactor with computational fluid dynamics software could provide a better comprehension of the local phenomena occurring, and so enable optimization of the contactor design for a better transfer.

To determine the overall transfer coefficient $K_L a$, experiments were carried out with recirculation of the liquid (see Figure 1) to better visualize the increase in dissolved ozone concentration during the transitional regime. Pure water buffered at acid pH was used to avoid decomposition of the molecular ozone into hydroxyl radicals. We note that pH variation from 1 to 9 does not impact the $K_L a$ value (Ferre-Aracil et al., 2015; Kuosa and Kallas, 2010). The material balance is described below; the notation is presented in Figure 4.

Figure 4. Simplified scheme of the process for $K_L a$ determination.

The mass balance in the tank cannot be neglected to determine $K_L a$ as in Equations 9 and 10.

$$Q_{\text{liq}} C_2 dt = Q_{\text{liq}} C_1 dt + V_{\text{tank}} dC_1 , \quad [9]$$

$$Q_{\text{liq}} (C_2 - C_1) dt = V_{\text{tank}} dC_1 , \quad [10]$$

where Q_{liq} is the liquid flowrate, C_1 is the dissolved ozone concentration at the membrane contactor inlet, C_2 is the dissolved ozone concentration at the membrane contactor outlet, and V_{tank} is the volume of the feed tank, which is agitated.

The mass balance on the membrane contactor, where the ozone is transferred to the water, is then specified in Equation 11.

$$Q(C_2 - C_1) = K_{\text{L}} a \, V_{\text{c}} \, \Delta C , \quad [11]$$

where

$$\Delta C = C^* - \bar{C} = \frac{C_2^* - C_1^*}{\ln\left(\frac{C_2^*}{C_1^*}\right)} - \bar{C} \approx \frac{C_2^* - C_1^*}{\ln\left(\frac{C_2^*}{C_1^*}\right)} - C_1 . \quad [12]$$

Equation 13 was established by combining Equations 11 and 12. After integration, the overall transfer coefficient can be deduced (Equation 14). Initially, there is no dissolved ozone in the liquid phase (i.e., boundary condition is $C(t_0) = 0$).

$$K_{\text{L}} a \, V_c \, \Delta C \, dt = V_{\text{tank}} dC_1 , \quad [13]$$

$$\ln(C^* - C_1) = \frac{-K_{\text{L}} a \; V_c}{V_{\text{tank}}} t + \ln(C^*) . \quad [14]$$

The value of the ozone K_La in pure water with no reaction was found to be 1.412×10^{-1} s^{-1}, neglecting the coefficient for the decomposition of molecular ozone into hydroxyl radicals owing to the acid pH of the water (pH = 3). The decomposition coefficient kc at this pH is 4×10^{-4} s^{-1} (Roth and Sullivan, 1981). In conventional ozonation processes, K_La is estimated at between 5×10^{-3} and 2.7×10^{-2} s^{-1} (for bubble columns) (Beltrán et al., 1997; Roustan et al., 1996). The mass transfer obtained in this study is therefore better than with bubble columns.

The specific exchange surface a, calculated from the volume of liquid in the shell of the contactor and the effective exchange surface, is about 2948 $m^2.m^{-3}$. Therefore, K_L was estimated to be 4.789×10^{-5} $m.s^{-1}$. Taking into account kc, K_L is 4.775×10^{-5} $m.s^{-1}$, only 0.3% of relative deviation compared to the previous value.

This value is higher than those presented by Pines et al. for a similar Reynolds number (about 400), which were about 2×10^{-5} $m.s^{-1}$ depending on the membrane material used (Pines et al., 2005). However, Pines et al. presented higher values of K_L at higher Reynolds numbers (e.g., $K_L = 7.6 \times 10^{-5}$ $m.s^{-1}$ at Re = 2000). This result proves the presence of a significant transfer resistance on the liquid side and highlights the importance of the reduction of liquid film thickness, with, for example, a greater turbulence, to optimize the ozone transfer.

Owing to the membrane resistance and to the low pressure difference between the two phases, K_L obtained with bubble reactors is lower than K_L obtained with membrane contactors (Leiknes et al., 2005). However, the main advantage of this new process is the specific exchange surface (a, in $m^2.m^{-3}$) which is particularly high in a membrane contactor. Consequently, the mass transfer K_La remains competitive with conventional processes. To achieve a larger specific exchange surface, a large quantity of membrane is required, leading to a high membrane construction cost before the ozonation process can be set up. However, a significantly lower operating cost is expected after the installation owing to the gas recycling. Because higher consumption of the produced ozone is achieved, less ozone needs to be generated (ozone production is expensive), and an ozone destructor is no longer needed (Stylianou et al., 2015b). In addition, the gas is supposed to be dry at the outlet of the contactor and then could be injected in the ozone generator. In this study, recycling the residual ozone at the gas outlet could lead to an economy of production of about 10 $g.Nm^{-3}$ of gaseous ozone and should have been complemented with newly generated ozone to achieve the desired concentration.

The overall transfer coefficient K_L depends mostly on the liquid flow conditions. As a consequence, this coefficient will be used later to study the ozone transfer with a reaction (i.e., chemical reaction

with organic matter, such as a dye or organic micropollutants or decomposition of molecular ozone), both in open and closed liquid circulation and at the same liquid flowrate.

3.2. Determination of the membrane transfer coefficient and of the resistance induced by the membrane

The membrane transfer coefficient was determined by the method described in Section 2.4. The intermediate calculations and the final value of k_m are presented in Table 2 and compared with the results obtained in the study of Bamperng et al (Bamperng et al., 2010).

Table 2. Comparison of membrane mass transfer coefficients.

The diffusivity of ozone in the membrane obtained in this work was one order of magnitude lower than in the study of Bamperng et al., even for a similar material (PTFE). This emphasizes the importance of the structural material used. More specifically, these results showed the impact of the membrane thickness on the ozone transfer in the membrane. The porosity and the pore diameter were higher in this work, and still led to a lower final transfer coefficient. The notable difference between the k_m values obtained can therefore be explained by the thickness difference.

Considering the overall resistance $R_{ov} = \frac{1}{K_L} = R_g + R_m + R_l$, the membrane resistance (R_m) and the part of the overall resistance due to the membrane (R_m/R_{ov}) were calculated from Equation 4. The membrane resistance was found to be 1.87×10^2 s.m^{-1}, less than 1% of the overall resistance. This percentage is the same as that found by Hasanoğlu et al. in their work on ammonia extraction with a hollow fiber membrane contactor (Hasanoğlu et al., 2013). By contrast, Khaisri et al. estimated this percentage at 40% in their study on CO_2 absorption with a PTFE hollow fiber membrane contactor (Khaisri et al., 2009). However, they assumed that membrane pores were partially wetted, leading to a higher membrane resistance than with non-wetted pores. The authors also compared three different membrane materials – PTFE, PP (polypropylene), and PVDF (polyvinylidene fluoride). The lowest membrane resistance was obtained for the PTFE material. We note that the method used to determine membrane resistance was not the same as in our work (the Wilson plot method was used).

In this study, due to the low proportion of the membrane in the overall resistance, the impact of the membrane thickness on the overall resistance is very restricted because of the dominating liquid side resistance. However, Bein et al. highlighted in a previous study that if it was generally the case for the hydrophobic fluoropolymers, it was not for inorganic or hydrophile materials like for instance for PDMS (polydimethylsiloxane), hydrophile PVDF, or α-Al_2O_3 (Bein et al., 2021). With these materials,

the membrane resistance can be significant, and thus the membrane thickness become a key parameter.

In addition, the resistance in the gas phase could be neglected relative to the resistance in the liquid phase, owing to the ozone diffusion coefficient in the gas phase, which is 4 orders of magnitude higher than in the water ($D_{\text{Dissolved O3,w}}$ = 1.708 × 10^{-9} $m^2.s^{-1}$ at 20 °C (Johnson and Davis, 1996), $D_{O3,g}$ = 1.00 × 10^{-5} $m^2.s^{-1}$ at 20 °C (Bamperng et al., 2010)). Therefore, most of the mass transfer resistance is on the liquid side, highlighting the key role of the liquid flow when using a membrane contactor for a gas liquid absorption application. This result agrees with the conclusion of Phattaranawik et al. in their study on mass transfer in a flat-sheet membrane contactor with ozonation: the ozone mass transport is controlled by the mass transfer resistance in the liquid film (Phattaranawik et al., 2005).

3.3. Study of the ozonation of pure water through a membrane contactor: impact of several variables on the ozone transfer

The analysis of the experimental data obtained with a 2^3 factorial design of experiments (DOE) was conducted to compare the significance and the impact of three variables on the ozone transfer, namely the liquid flow rate (Q_{liq}), the gas flow rate (Q_{gas}), and the ozone concentration at the inlet to the gas phase (C_{O3}). The DOE described in Table 3 was first followed. The experiments were carried out with the liquid phase in open circuit.

Table 3. DOE for the study of ozone transfer in buffered pure water.

The mean response obtained for each experiment, corresponding to the ozone transferred from the gas phase to the liquid phase, was plotted on the Figure 5. This dose was calculated using two different methods. The first was a mass balance on the gas phase (i.e., the difference between the quantity of ozone at the inlet and at the outlet of the membrane contactor). The second was the determination of the dissolved ozone concentration in the liquid phase. Each experiment was at least duplicated, and the error bars correspond to the standard deviations.

Systematically, experiments were conducted at acid pH using a buffered solution (see Section 2.3), thus avoiding the decomposition of molecular ozone into hydroxyl radical. Pure water was used (TOC < 200 ppb), thus avoiding the reaction of dissolved ozone with substances in the liquid phase. Consequently, the result (i.e., the transferred ozone) is expected to be the same whichever method is used. Consistent results were obtained with the two methods. The method of the mass balance on the gas phase was chosen for the statistical analysis of the data.

Figure 5. Transferred ozone calculated by mass balance on the gas phase vs by mass balance on the liquid phase.

A linear model was used for the interpretation of these results. The Pareto chart, where dominating and influential factors can be deduced, was plotted using Minitab 19 Statistical software on the Figure 6 (Wenten et al., 2012). Terms with longer bars have more influence on the response. The red line is the effect size at the 0.10 level of significance. Grey bars represent non-significant terms that were removed from the model. The response was the dose of ozone transferred by mass balance on the gas phase. The results showed that the three factors studied (liquid flow rate (A), gas flow rate (B), and ozone concentration at the gas inlet (C)) were influential on the dose of transferred ozone. Only the interaction factor between the liquid flow rate and the ozone concentration at the gas inlet had a significant influence on the response. Liquid flow rate was the variable with the most influence, followed by ozone concentration at the gas inlet rate, then gas flow rate and finally liquid flow coupled with ozone concentration.

Figure 6. Pareto Chart of Standardized Effects (Response is dose of transferred ozone; α = 0.1).

To maximize the dose of transferred ozone, the optimal factor settings were Qliq = 75 L/h, Qgas = 30 L/h and CO$_3$gas = 30 g/Nm^3. Under these conditions, the predicted dose of transferred ozone with the adjusted quadratic model was 2.96 × 10^{-5} g/s. The regression equation of the dose of transferred ozone is defined in Equation 15, and explains 96.36% of the variation of the dose transferred (i.e., R^2 = 96.36%).

$$\text{Dose transferred } (\times 10^5) = -0.18 + 0.0066\ Qliq + 0.02295\ Qgas - 0.0649\ CO_3gas + 0.001735\ (Qliq \times CO_3gas), \quad [15]$$

where Dose transferred is the dose of ozone transferred from the gas phase to the liquid phase by mass balance on the gas phase (in g/s, multiply the result by 10^{-5}), Qliq is the liquid flow rate (in L/h), Qgas is the gas flow rate (in L/h), and CO$_3$gas is the ozone concentration at the inlet to the gas phase (in g/Nm^3)

The model was also checked by analysis of the residuals, and no unusual data point was found.

3.4. Study of the ozonation of Acid Orange 7 (AO7) through the membrane contactor: acceleration factor

The experiments with pure water recirculating enabled the determination of the ozone K_La in the membrane contactor, which is the same when the liquid phase is not pure water (for identical liquid flow conditions). To study the impact of an irreversible chemical reaction on the ozone transfer, Acid Orange 7 (AO7), a dye highly reactive to molecular ozone (k_{O3} = 1.20 x 10^4 M^{-1}.s^{-1}), was selected. The

effects of operating conditions on mass transfer performance were investigated in the previous section and enabled the choice of appropriate conditions for dye removal (i.e., AO7 abatement). Experiments with AO7 solution were carried out, at an initial concentration of about 5 $mg.L^{-1}$. Material balances established in Section 3.1. could not be easily resolved with the presence of a reaction, mainly because the reaction took place not only in the membrane contactor but also inside the tank. Several variables therefore depended on time. The study of AO7 removal was thus conducted with water in an open loop (i.e., there was no recirculation of the liquid phase in the membrane contactor). In this process, ozone was transferred from the gas phase to the liquid phase through the membrane. Once dissolved, it reacted with the dye in the solution. Comparison between pure water and dye experiments carried out with liquid in the open loop showed a higher ozone transfer in the presence of AO7 (1.27 $g.h^{-1}.m^{-2}$ instead of 0.84 $g.h^{-1}.m^{-2}$ with buffered water), indicating the existence of an acceleration factor due to the decoloring reaction. This can be explained by the steepened concentration gradient due to the reaction with the dissolved ozone.

The reaction can be described by Equation 16 where b is the stoichiometric coefficient of the reaction.

$$O_{3\,(L)} + b\ AO7_{(L)} \rightarrow \text{Products} \quad [16]$$

Molecular ozone could also react with degradation by-products of AO7. However, the low residence time (< 2 s) in the contactor, combined with the high reaction constant of AO7 with O_3, make the theoretical reactions that could ensue negligible.

As seen previously (see Section 2.4), the mass transfer mechanism in the membrane contactor is divided into several regions (see Figure 3). The objective was here to identify where the reaction took place and whether it had any impact on the mass transfer. To identify the reaction regime during the reaction between AO7 and dissolved ozone, the Hatta number was calculated.

$$\text{Ha} = \frac{\sqrt{k_2\, C_{\text{AO7\_lm}} D_{\text{Dissolved O3-Water}}}}{k_L}, \quad [17]$$

where k_2 is the 2nd order reaction constant of AO7 with dissolved ozone (= 1.20×10^4 $M^{-1}.s^{-1}$ (Gomes et al., 2010)), C_{AO7_lm} is the logarithmic mean of the AO7 concentration at the inlet and at the outlet of the reactor (= 1.216 x 10^{-5} $mol.L^{-1}$), $D_{\text{Dissolved O3-Water}}$ is the diffusivity of dissolved ozone in the water (= 1.708×10^{-9} $m^2.s^{-1}$ at 20 °C (Johnson and Davis, 1996)), and k_L is the liquid transfer coefficient ≈ K_L because of the low membrane and gas resistances (= 4.789×10^{-5} $m.s^{-1}$, see Section 3.1)

The Hatta number was found to be 0.33. According to Roustan, this corresponds to a moderately fast reaction, which takes place partially in the liquid film and partially in the liquid bulk (Roustan, 2003).

The most suitable reactor to promote this type of reaction has a high interfacial area and a high liquid retention time. In this work, the use of hollow fibers gave a high interfacial area, but the liquid retention time was very short (1.7 s). The use of a lower liquid flowrate would probably have improved the reaction between dissolved ozone and AO7 in the liquid bulk, thus yielding a better AO7 abatement.

The acceleration factor (*E*) corresponds to the ratio of the material flow transferred at the gas/liquid interface without a chemical reaction to that with a chemical reaction. Ha was found to exceed 0.3, implying E > 1. For a second order reaction (i.e., $r = kC_{O3}C_{AO7}$), *E* could be determined with precision and is defined as:

$$E = \frac{\mathrm{Ha}\sqrt{\frac{E_{\mathrm{AL}}-E}{E_{\mathrm{AL}}-1}}}{\tanh\left[\mathrm{Ha}\sqrt{\frac{E_{\mathrm{AL}}-E}{E_{\mathrm{AL}}-1}}\right]} \quad , [18]$$

where E_{AL} is called the "limit acceleration factor", and is described by Equation 19.

$$E_{\mathrm{AL}} = 1 + \frac{D_{\mathrm{AO7,w}}\, C_{\mathrm{AO7\_lm}}}{\mathrm{b}\, D_{\mathrm{Dissolved\ O3,w}}\, C_{\mathrm{Dissolved\ O3\_I}}} \quad , [19]$$

where $D_{AO7,w}$ is the diffusivity of AO7 in the water (= 8.48 × 10^{-10} $m^2.s^{-1}$ at 20 °C (Hori et al., 1987)), and $C_{Dissolved\ O3\_I}$ is the concentration of dissolved ozone at the gas/liquid interface (= 1.55 × 10^{-4} $mol.L^{-1}$ according to the Henry's law).

Solving Equation 18, the acceleration factor was calculated to be 1.03. This result implies that the ozone mass transfer was slightly accelerated by the reaction between AO7 and dissolved ozone, and that the resistance on the liquid side was slightly lower in the presence of AO7 than without (i.e., lower with chemical absorption than with physical absorption) (see Section 2.4).

To compare the AO7 abatement obtained using the membrane contactor with a conventional process, experiments were conducted with a bubble column (see Section 2.2). The initial AO7 concentration was approximately the same as in the membrane contactor experiments (i.e., about 5 $mg.L^{-1}$). The average abatement obtained with the membrane contactor (i.e., 34%) in a very short residence time (i.e., < 2 s) was achieved in over 3 minutes with the bubble column (and 100% decoloring was achieved in 11 min on average). The membrane contactor therefore holds promise, but it must be noted that although the applied ozone fluxes in $g.h^{-1}$ were close in the membrane contactor and in the bubble column experiments, both applied ozone flow and transferred ozone flow in $g.h^{-1}._{treated}L^{-1}$ were significantly higher in the membrane contactor experiments, largely explaining the marked difference between the residence time of the two reactors to achieve 34% AO7 abatement (see Table 4).

Table 4. Comparison between membrane contactor and bubble column for AO7 removal.

In Table 4, an average of the result obtained is given (experiments had been performed in triplicate with the membrane contactor and in duplicate with the bubble reactor). The associated standard deviation is also indicated. We see that the applied ozone flow in the membrane contactor experiments was 89 times higher than in the conventional process experiment. The AO7 concentration time course obtained with the bubble column showed that AO7 abatement was proportional to the time. We can therefore assume that with an applied ozone flow of 6.596 $g.h^{-1}._{treated}L^{-1}$ (i.e., 89 × 0.074 $g.h^{-1}._{treated}L^{-1}$), a residence time of 2.5s (+/- 0.9s) (i.e., 3.70 / 89 min) would be required to achieve 34% AO7 abatement in the bubble column, which is 43% superior to the time necessary with the membrane contactor to reach the same efficiency.

Impact of ozone on membrane material

After about 40 hours of exposition to ozone environment, despite correct transmembrane pressures (in particular the breakthrough pressure, see Section 2.1), a large volume of liquid was observed on the gas side. This time corresponded to the circulation of about 10 g of ozone gas through the contactor. This value was estimated by cumulating, for all the experiments, the mass flow rate in the gas phase at the inlet to the contactor. The same problem occurred for several membrane contactors that were similar (same material, number of fibers, and supplier). Once watertightness was lost, large volumes of water were found at the gas outlet in each experiment. The membrane contactor was therefore replaced.

Several hypotheses can explain the presence water in the gas outlet. First, a large amount of water may have flowed through the membrane pores and then circulated inside the fibers to the gas outlet. A smaller amount might not be visible but would also affect the ozone transfer. The presence of water in the pores, even partial, is a major problem because it significantly reduces the transfer of ozone from the gas to the liquid phase owing to the lower diffusivity of ozone in the liquid than in the gas phase (see Section 3.2). This could have happened if the breakthrough pressure had been locally exceeded, for example through a change in water flow or in hydrophobicity. Visually, it was not possible to check partial or complete penetration of water inside the membrane pores during the experiments. However, liquid was in these cases visible at the gas outlet.

Another hypothesis is a loss of seal at the potted part, which is where fibers are bonded in place using resin, joining the shell to the fibers. The potting of a membrane contactor, particularly if it is for an ozonation or oxidation application, is a difficult process because it must fulfill several requirements. First, the resin must adhere to the membrane material used, and PTFE is notably

adhesion-resistant. The resin must also be durable. Here, fibers all came unstuck on one side of the contactor. This last hypothesis was therefore taken as most probable.

A test validated that the potting was no longer sealed and watertight. The resin used for the potting of the membrane contactors used in this work was polyurethane resin. It proved not to resistant attack by ozone over time. Polyurethane resin is considered to have a good ozone resistance (Irfan, 1998). However, Sleeper and Henry showed in their tests on durability of materials exposed to ozone that polyurethane sealant was immediately degraded by ozone. Some research is reported in the literature on the production of specific products for this field. For instance, a patent has been filed for making a polyurethane resin specifically for use with ozone (Yoon et al., 2011).

It was also notable that fibers came unstuck on only one side (the gas outlet), which is the side where there was the lowest dissolved ozone concentration and gaseous ozone concentration. No explanation was found for this particularity. One hypothesis is the transmembrane pressure, which was checked at the inlet and at the outlet of the contactor, but which could locally exceed the breakthrough pressure. The water enters the contactor perpendicularly. This could potentially explain the presence of water (and of dissolved ozone) inside the fibers on this side. As observed by other authors, dissolved ozone is more aggressive toward materials than gaseous ozone, which could explain why this side was attacked first (Sleeper and Henry, 2002). With time, fibers would come off on both sides.

To evaluate the deterioration of the fiber properties over time and to determine whether this deterioration could favor water penetration inside, analysis of hydrophobicity and material structure was carried out by contact angle measurements and SEM images.

The following SEM images (Figure 7) show the tested samples according to their location, both for outer surface and lumen of samples, with several magnifications.

Figure 7. SEM images of an inner fiber sample of the bundle at different locations for lumen side and outer surface.

Figure 7 shows that the lumen side was less damaged than the outer surface for every location in the contactor. These results suggest there was very little reaction between the ozone and the membrane material inside the fibers. Material balances could therefore be established without taking into account the presence of a reaction between gaseous ozone and the material. Conversely, the outer surfaces of fibers were particularly damaged, especially in the middle of the contactor. A torn crust was visible, which could induce a modification of the membrane porosity and so could explain the water penetration inside the fibers. There was clearly some reaction between the ozone and the

membrane material on the outer surface. According to Fujimoto et al., peroxides are formed on the PDMS surface when ozone is in the presence of water (Fujimoto et al., 1993; Zoumpouli et al., 2018). However, according to the authors (Fujimoto et al.), this does not occur on a Teflon surface, and therefore should not happen on a PTFE surface. The difference between the results obtained (i.e., for the lumen side and for the outer surface of the fiber) could thus be explained by the greater aggressivity of the dissolved ozone relative to gaseous ozone (Sleeper and Henry, 2002).

Contact angles were investigated on the same samples as previously. Importantly, the values obtained were qualitative but not quantitative, so must be considered with caution. The contact angles measured with the analytical method used (see Section 2.1) depended on the porosity, roughness, and hydration state of the membrane. This method is ill-adapted to a non-planar surface such as the hollow fiber in this work (porous hollow fiber membrane). However, by depositing a very small volume of water on the surface to be analyzed, the material being hydrophobic, contact angles were measured without being exactly quantified. Contact angle measurements revealed no alteration of the membrane hydrophobicity whatever the location of the sample. A change in the membrane hydrophobicity did not therefore account for the penetration of a large volume of water inside fibers.

To conclude, the factor limiting the use of the membrane contactor over time seems to be the potting, particularly the resin used to bond the fibers. The loss of adhesion of the fibers inside the resin explains the loss of seal after a period of ozonation. However, the membrane material also presented significant alterations over time, specifically on the outer surface of the fibers, which was in contact with dissolved ozone. According to the literature, PTFE is one of the best polymeric materials for resisting ozonation over time (Bein et al., 2021). Bamperng et al. observed no modification of the PTFE after more than 16 hours of exposure to an ozone environment concentrated at 40 $g.Nm^{-3}$ (Bamperng et al., 2010). Santos et al. had the same observation for an ozone exposure of 5.25 $g.h^{-1}$ during 4 hours, corresponding to 21 g of ozone, which is twice the amount achieved in this study (Alves dos Santos et al., 2015). However, their study was made with gaseous ozone, which is supposed to be less aggressive than dissolved ozone (Sleeper and Henry, 2002). Furthermore, Bein et al. suggested that even if no changes have already been reported for PTFE, unlimited stability cannot be guaranteed in the case of a long-term exposure due to the scarcity of the existing data and to the problems of chemical stability reported in the case of harsh conditions, like for instance defluorination during chemical cleaning (Bein et al., 2021). According to the SEM images presented in this work (Figure 7), PTFE material could not be suitable for membrane contactors in practical application of ozonation. The study of another material, such as PVDF, also

known for being resistant to ozone oxidation, would be useful to compare results. However, in a previous study, Bamperng et al. compared PTFE and PVDF and observed for this last a significant reduction of the mass transfer of 30% over 16h at the same ozone concentration (40 $g.Nm^{-3}$) (Bamperng et al., 2010). Previous studies have recently pointed out the unsuitability of polymeric membranes for treatment involving oxidizing agents such as ozone (Shanbhag et al., 1998). Some research on ozonation with ceramic (i.e., chemically inert) membrane contactors has been conducted (Heng et al., 2007; Jansen et al., 2005; Stylianos et al., 2015b). However, the production of ceramic membranes in the form of hollow fibers (very small diameter fiber in order to obtain the largest possible exchange surface area) is still being developed (Dashti and Asghari, 2015). In addition, ceramic membranes are generally more hydrophilic than the polymerics, and thus water could more easily penetrate in the pores and decrease the mass transfer in the case of a porous membrane. The addition of a hydrophobic layer could be a solution (Stylianou et al., 2015a). Nevertheless, no study has been made at this time about the chemical stability of these layers after a long-term exposure to ozone (Bein et al., 2021). Simultaneously, the use of nonporous membranes (ceramic or polymeric) could avoid the transmembrane pressure problem (i.e., the requirement not to exceed the breakthrough pressure and the bubble pressure). One disadvantage would be the higher mass transfer resistance using dense membranes compared to porous membranes owing to their higher membrane resistance. However, Pines et al. demonstrated in their work that the overall mass transfer was not necessarily lower with nonporous membranes than with polymeric membranes (Pines et al., 2005). Another solution would be to use composite membranes with a porous support and a dense layer. This would eliminate any problem of transmembrane pressure while reducing membrane resistance thanks to the porous part (compared with dense membranes) (Chabanon, 2012; Favre and Roizard, 2012). Finally, one other solution could be to deposit a thin layer of an ozone-resistant material around the hollow fibers, for example by soaking, on the potted part of the contactor to prevent fiber detachment.

4. Conclusion

This study set out to gain more knowledge on the ozonation process using an in/out membrane contactor. A full characterization was performed using water and a model pollutant. The main conclusions are as follows:

- The overall mass transfer coefficient $K_L a$ measured in this study showed that the membrane contactor is an advantageous device for ozonation compared with conventional processes,

despite the addition of a resistance to the mass transfer (i.e., the membrane resistance), particularly because of its large specific exchange surface area.

- The mass transfer resistance due to the membrane depends on the material used. It represents less than 1% of the overall resistance. The $K_L a$ value therefore depends mainly on the liquid flow conditions.
- The main variables that have an impact on the ozone transfer are the ozone concentration in the gas phase and the liquid flowrate. Conversely, gas flowrate has very little impact on the ozone transfer.
- The results obtained with AO7 solutions prove that the membrane contactor can be effective for organic pollutant ozonation, even at very short contact times.
- When a chemical reaction takes place in the liquid, an acceleration of the ozone transfer occurs, owing to the steepened concentration gradient. The presence of organic micropollutants could therefore favor ozone transfer through a membrane contactor.

This work is a preliminary study for the ozonation of organic micropollutants with membrane contactors in the same process configuration.

Acknowledgments

The authors thank Didier Cot for SEM images and Thierry Thami for contact angle measurements (European Institute of Membranes).

This research did not receive any specific grants from funding agencies in the public, commercial, or not-for-profit sectors.

References

Alves dos Santos, F.R., Borges, C.P., da Fonseca, F.V., 2015. Polymeric Materials for Membrane Contactor Devices Applied to Water Treatment by Ozonation. Mater. Res. 18, 1015–1022. https://doi.org/10.1590/1516-1439.016715

Atchariyawut, S., Phattaranawik, J., Leiknes, T., Jiraratananon, R., 2009. Application of ozonation membrane contacting system for dye wastewater treatment. Sep. Purif. Technol. 66, 153–158. https://doi.org/10.1016/j.seppur.2008.11.011

Bader, H., Hoigné, J., 1982. Determination of Ozone In Water By The Indigo Method: A Submitted Standard Method. Ozone Sci. Eng. J. Int. Ozone Assoc. 4, 169–176. https://doi.org/10.1080/01919510390481531

Bamperng, S., Suwannachart, T., Atchariyawut, S., Jiraratananon, R., 2010. Ozonation of dye wastewater by membrane contactor using PVDF and PTFE membranes. Sep. Purif. Technol. 72, 186–193. https://doi.org/10.1016/j.seppur.2010.02.006

Bein, E., Zucker, I., Drewes, J.E., Hübner, U., 2021. Ozone membrane contactors for water and wastewater treatment: A critical review on materials selection, mass transfer and process design. Chem. Eng. J. 413. https://doi.org/10.1016/j.cej.2020.127393

Beltrán, F.J., García-Araya, J.F., Encinar, J.M., 1997. Henry and mass transfer coefficients in the ozonation of wastewaters. Ozone Sci. Eng. 19, 281–296. https://doi.org/10.1080/01919519708547307

Bolong, N., Ismail, A.F., Salim, M.R., Matsuura, T., 2009. A review of the effects of emerging contaminants in wastewater and options for their removal. Desalination 239, 229–246. https://doi.org/10.1016/j.desal.2008.03.020

Chabanon, E., 2011. Contacteurs à membranes composites et contacteurs microporeux pour procédés gaz-liquide intensifiés de captage du CO2 en post-combustion : expérimentation et modélisation. Génie des procédés. École Nationale Supérieure des Mines de Paris : thèse de doctorat. Français. <NNT : 2011ENMP0061>. <pastel-00677145>

Dashti, A., Asghari, M., 2015. Recent Progresses in Ceramic Hollow-Fiber Membranes. ChemBioEng Rev. 2, 54–70. https://doi.org/https://doi.org/10.1002/cben.201400014

Favre, D., Roizard, E., 2012. Conception et étude de contacteurs gaz/liquide à peau dense pour le captage du dioxyde de carbone - Une étape importante pour l'intensification du captage en postcombustion. Tech. Ing. Base documentaire : TIB495DUO. Ref. article : re166.

Ferre-Aracil, J., Cardona, S.C., Navarro-Laboulais, J., 2015. Determination and validation of Henry's constant for ozone in phosphate buffers using different analytical methodologies. Ozone Sci. Eng. 37, 106–118.

Fujimoto, K., Takebayashi, Y., Inoue, H., Ikada, Y., 1993. Ozone-induced graft polymerization onto polymer surface. J. Polym. Sci. Part A Polym. Chem. 31, 1035–1043. https://doi.org/10.1002/pola.1993.080310426

Gabelman, A., Hwang, S.T., 1999. Hollow fiber membrane contactors. J. Memb. Sci. 159, 61–106. https://doi.org/10.1016/S0376-7388(99)00040-X

Gogoi, A., Mazumder, P., Tyagi, V.K., Tushara Chaminda, G.G., An, A.K., Kumar, M., 2018. Occurrence and fate of emerging contaminants in water environment: A review. Groundw. Sustain. Dev. 6, 169–180. https://doi.org/10.1016/j.gsd.2017.12.009

Gomes, A.C., Nunes, J.C., Simões, R.M.S., 2010. Determination of fast ozone oxidation rate for textile dyes by using a continuous quench-flow system. J. Hazard. Mater. 178, 57–65. https://doi.org/10.1016/j.jhazmat.2010.01.043

Guillossou, R., Le Roux, J., Brosillon, S., Mailler, R., Vulliet, E., Morlay, C., Nauleau, F., Rocher, V., Gaspéri, J., 2020. Benefits of ozonation before activated carbon adsorption for the removal of organic micropollutants from wastewater effluents. Chemosphere 245. https://doi.org/10.1016/j.chemosphere.2019.125530

Hasanoğlu, A., Romero, J., Plaza, A., Silva, W., 2013. Gas-filled membrane absorption: A review of three different applications to describe the mass transfer by means of a unified approach. Desalin. Water Treat. 51, 5649–5663. https://doi.org/10.1080/19443994.2013.769603

Heng, S., Yeung, K.L., Djafer, M., Schrotter, J.-C., 2007. A novel membrane reactor for ozone water treatment. J. Memb. Sci. 289, 67–75. https://doi.org/10.1016/j.memsci.2006.11.039

Hori, T., Kamon, N., Kojima, H., Rohner, R.M., Zollinger, H., 1987. Structure correlation between diffusion coefficients of simple organic compounds and of anionic and cationic dyes in water. J. Soc. Dye. Colour. 103, 265–270. https://doi.org/10.1111/j.1478-4408.1987.tb01119.x

Irfan, M.H., 1998. Polyurethanes in the construction industry, in: Chemistry and Technology of Thermosetting Polymers in Construction Applications. Dordrecht, pp. 123–144.

Iversen, S.B., Bhatia, V.K., Dam-Johansen, K., Jonsson, G., 1997. Characterization of microporous membranes for use in membrane contactors. J. Memb. Sci. 130, 205–217. https://doi.org/10.1016/S0376-7388(97)00026-4

Jansen, R.H.S., de Rijk, J.W., Zwijnenburg, A., Mulder, M.H.V., Wessling, M., 2005. Hollow fiber membrane contactors—A means to study the reaction kinetics of humic substance ozonation. J. Memb. Sci. 257, 48–59. https://doi.org/10.1016/J.MEMSCI.2004.07.038

Johnson, P.N., Davis, R.A., 1996. Diffusivity of ozone in water. J. Chem. Eng. Data 41, 1485–1487. https://doi.org/10.1021/je9602125

Khaisri, S., deMontigny, D., Tontiwachwuthikul, P., Jiraratananon, R., 2009. Comparing membrane resistance and absorption performance of three different membranes in a gas absorption membrane contactor. Sep. Purif. Technol. 65, 290–297. https://doi.org/10.1016/j.seppur.2008.10.035

Khayet, M., Matsuura, T., 2001. Preparation and Characterization of Polyvinylidene Fluoride Membranes for Membrane Distillation. Ind. Eng. Chem. Res. 40, 5710–5718. https://doi.org/10.1021/ie010553y

Kukuzaki, M., Fujimoto, K., Kai, S., Ohe, K., Oshima, T., Baba, Y., 2010. Ozone mass transfer in an ozone-water contacting process with Shirasu porous glass (SPG) membranes-A comparative study of hydrophilic and hydrophobic membranes. Sep. Purif. Technol. 72, 347–356. https://doi.org/10.1016/j.seppur.2010.03.004

Kuosa, M., Kallas, J., 2010. Multicomponent reaction models in ozonation and reduction in the number of model parameters. J. Hazard. Mater. 183, 823–832. https://doi.org/10.1016/j.jhazmat.2010.07.101

Leiknes, T., Phattaranawik, J., Boller, M., Von Gunten, U., Pronk, W., 2005. Ozone transfer and design concepts for NOM decolourization in tubular membrane contactor. Chem. Eng. J. 111, 53–61. https://doi.org/10.1016/j.cej.2005.05.007

Luo, Y., Guo, W., Ngo, H.H., Nghiem, L.D., Hai, F.I., Zhang, J., Liang, S., Wang, X.C., 2014. A review on the occurrence of micropollutants in the aquatic environment and their fate and removal during wastewater treatment. Sci. Total Environ. 473–474, 619–641. https://doi.org/10.1016/j.scitotenv.2013.12.065

Margot, J., Kienle, C., Magnet, A., Weil, M., Rossi, L., de Alencastro, L.F., Abegglen, C., Thonney, D., Chèvre, N., Schärer, M., Barry, D.A., 2013. Treatment of micropollutants in municipal wastewater: Ozone or powdered activated carbon? Sci. Total Environ. 461–462, 480–498. https://doi.org/10.1016/j.scitotenv.2013.05.034

Mavroudi, M., Kaldis, S.P., Sakellaropoulos, G.P., 2006. A study of mass transfer resistance in membrane gas–liquid contacting processes. J. Memb. Sci. 272, 103–115. https://doi.org/10.1016/J.MEMSCI.2005.07.025

Merle, T., Pronk, W., Von Gunten, U., 2017. MEMBRO 3 X, a Novel Combination of a Membrane Contactor with Advanced Oxidation (O 3 /H 2 O 2) for Simultaneous Micropollutant Abatement and Bromate Minimization. Environ. Sci. Technol. Lett 4, 13. https://doi.org/10.1021/acs.estlett.7b00061

Nguyen, P.T., 2011. Contacteurs à membranes denses pour les procédés d'absorption gaz-liquide intensifiés : application à la capture du CO 2 en post combustion. Thèse de doctorat. Institut National Polytechnique de Lorraine. Français.

Pabby, A.K., Sastre, A.M., 2013. State-of-the-art review on hollow fibre contactor technology and membrane-based extraction processes. J. Memb. Sci. 430, 263–303. https://doi.org/10.1016/j.memsci.2012.11.060

Phattaranawik, J., Leiknes, T., Pronk, W., 2005. Mass transfer studies in flat-sheet membrane contactor with ozonation. J. Memb. Sci. 247, 153–167. https://doi.org/10.1016/j.memsci.2004.08.020

Pines, D., Min, K.-N., J. Ergas, S., Reckhow, D., 2005. Investigation of an Ozone Membrane Contactor System. https://doi.org/10.1080/01919510590945750

Prieto-Rodríguez, L., Oller, I., Klamerth, N., Agüera, A., Rodríguez, E.M., Malato, S., 2013. Application of solar AOPs and ozonation for elimination of micropollutants in municipal wastewater treatment plant effluents. Water Res. 47, 1521–1528. https://doi.org/10.1016/j.watres.2012.11.002

Roth, J.A., Sullivan, D.E., 1981. Solubility of ozone in water 137–140.

Roustan, M., 2003. Transferts gaz-liquide dans les procédés de traitement des eaux et des effluents gazeux. Éd. Tec & doc, Paris.

Roustan, M., Wang, R.Y., Wolbert, D., 1996. Modeling hydrodynamics and mass transfer parameters in a continuous ozone bubble column. Ozone Sci. Eng. 18, 99–115. https://doi.org/10.1080/01919519608547331

Schlüter-Vorberg, L., Prasse, C., Ternes, T.A., Mückter, H., Coors, A., 2015. Toxification by transformation in conventional and advanced wastewater treatment: the antiviral drug acyclovir. Environ. Sci. Technol. Lett. 2, 342–346. https://doi.org/10.1021/acs.estlett.5b00291

Schmitt, A., Mendret, J., Roustan, M., Brosillon, S., 2020. Ozonation using hollow fiber contactor technology and its perspectives for micropollutants removal in water: A review. Sci. Total Environ. vol. 729, p. 138664. https://doi.org/10.1016/j.scitotenv.2020.138664

Shanbhag, P. V, Guha, A.K., Sirkar, K.K., 1998. Membrane-Based Ozonation of Organic Compounds. Ind. Eng. Chem. Res. 37, 4388–4398. https://doi.org/10.1021/ie980182u

Sleeper, W., Henry, D., 2002. Durability Test Results of Construction and Process Materials Exposed to Liquid and Gas Phase Ozone. Ozone Sci. Eng. 9512, 249–260. https://doi.org/10.1080/01919510208901616

Snyder, S.A., Wert, E.C., Rexing, D.J., Zegers, R.E., Drury, D.D., 2006. Ozone oxidation of endocrine disruptors and pharmaceuticals in surface water and wastewater. Ozone Sci. Eng. 28, 445–460. https://doi.org/10.1080/01919510601039726

Stylianou, S. K., Sklari, S.D., Zamboulis, D., Zaspalis, V.T., Zouboulis, A.I., 2015a. Development of bubble-less ozonation and membrane filtration process for the treatment of contaminated water. J. Memb. Sci. 492, 40–47. https://doi.org/10.1016/j.memsci.2015.05.036

Stylianou, S. K., Szymanska, K., Katsoyiannis, I.A., Zouboulis, A.I., 2015b. Novel Water Treatment Processes Based on Hybrid Membrane-Ozonation Systems: A Novel Ceramic Membrane Contactor for Bubbleless Ozonation of Emerging Micropollutants. J. Chem. 2015, 1–12. https://doi.org/10.1155/2015/214927

Wang, R., Shi, L., Tang, C.Y., Chou, S., Qiu, C., Fane, A.G., 2010. Characterization of novel forward osmosis hollow fiber membranes. J. Memb. Sci. 355, 158–167. https://doi.org/10.1016/j.memsci.2010.03.017

Wenten, I.G., Julian, H., Panjaitan, N.T., 2012. Ozonation through ceramic membrane contactor for iodide oxidation during iodine recovery from brine water. Desalination 306, 29–34. https://doi.org/10.1016/j.desal.2012.08.032

Yoon, I., Jeon, I., Wi, O., Park, C., Hong, Y., 2011. Ozone resistant polyurethane composition and process of preparing same.

Zoumpouli, G., Baker, R., Taylor, C., Chippendale, M., Smithers, C., Xian, S., Mattia, D., Chew, J., Wenk, J., 2018. A Single Tube Contactor for Testing Membrane Ozonation. https://doi.org/10.3390/w10101416

Figures

Suggestions of presentation are highlighted in green.

Modifications after the first submission are highlighted in yellow.

Modifications after the 2nd submission are highlighted in blue.

Part 1. Figures

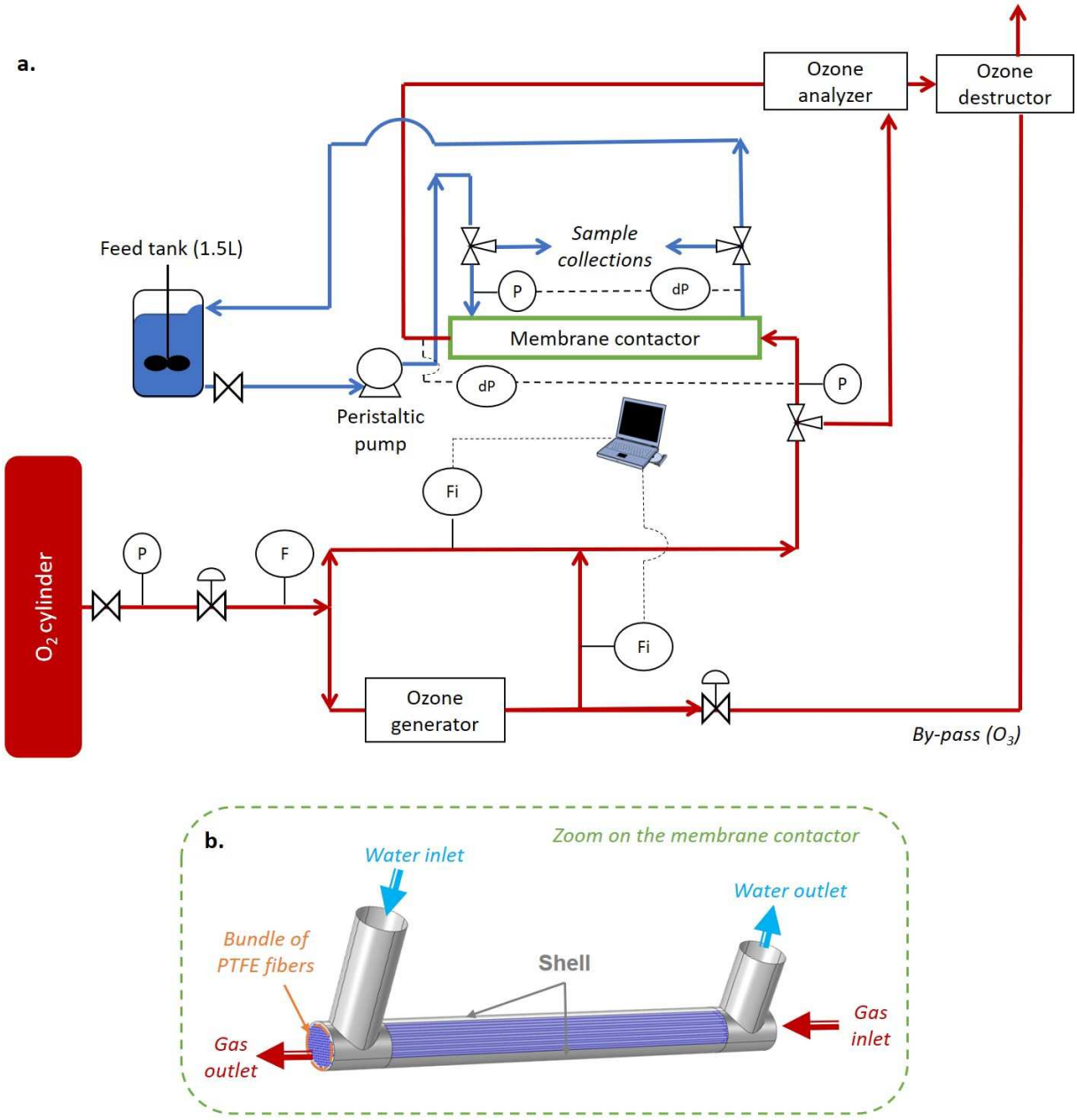

Figure 1. a. Flowsheet of the ozonation pilot - liquid in closed loop - gas in open circuit (red: gas stream, blue: liquid stream); b. Zoom on the configuration of the membrane contactor.

(1.5-column fitting image, or 2)

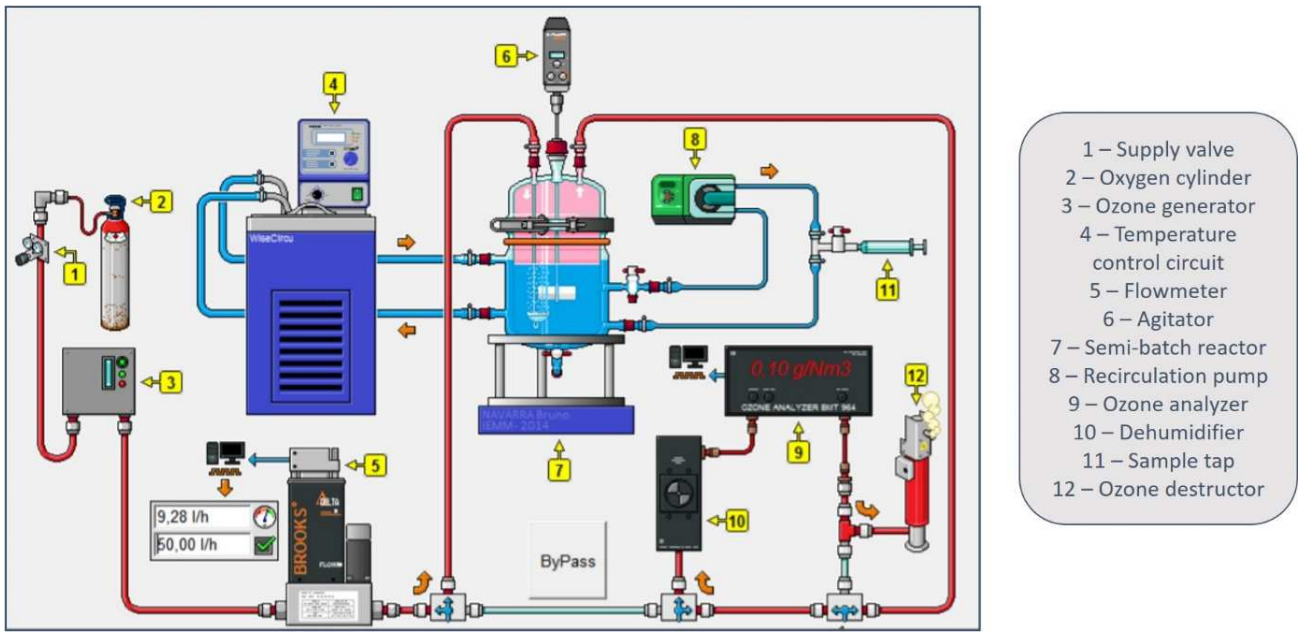

Figure 2. Scheme of the ozonation pilot with bubble column.

(2-column fitting image, or 1.5)

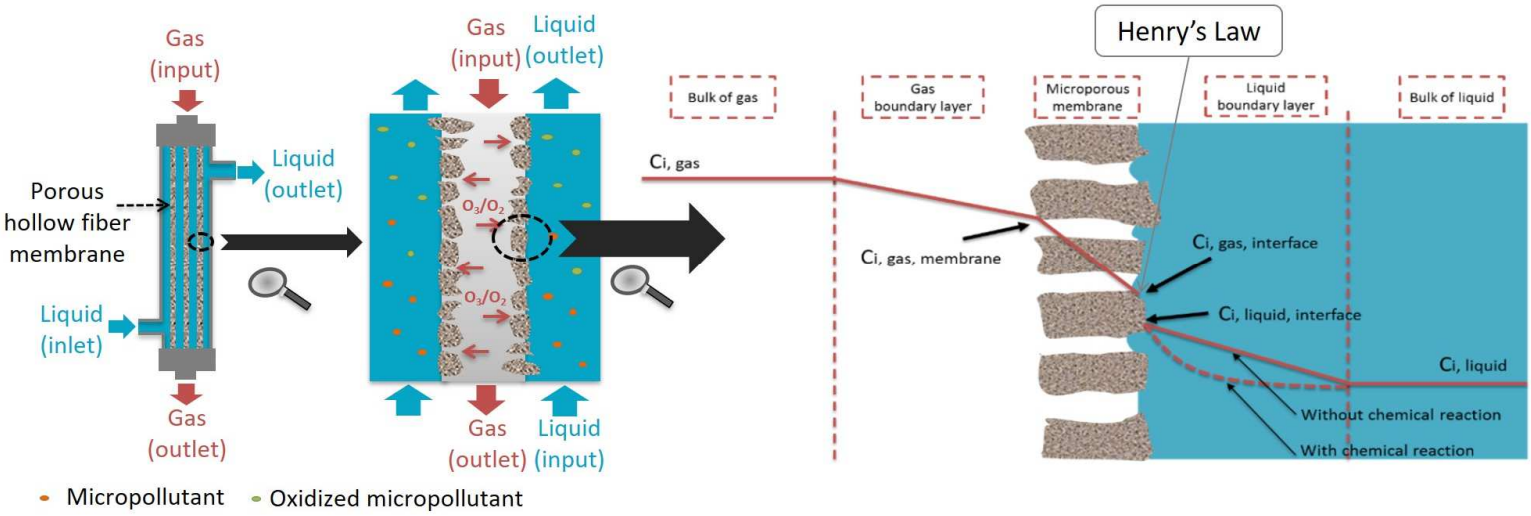

Figure 3. Ozone concentration profile in a membrane contactor (adapted from Schmitt et al., 2020).

(2-column fitting image)

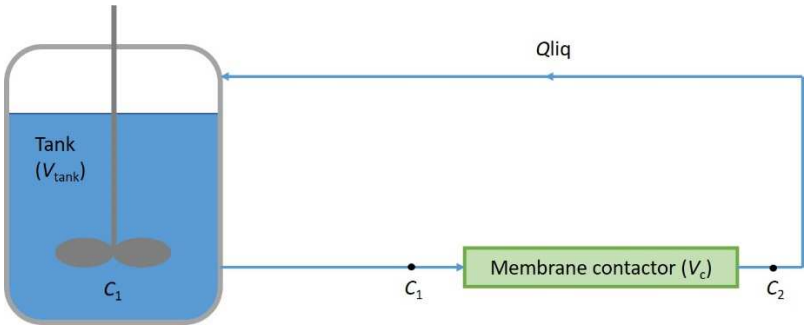

Figure 4. Simplified scheme of the process for K_La determination.

(1-column fitting image)

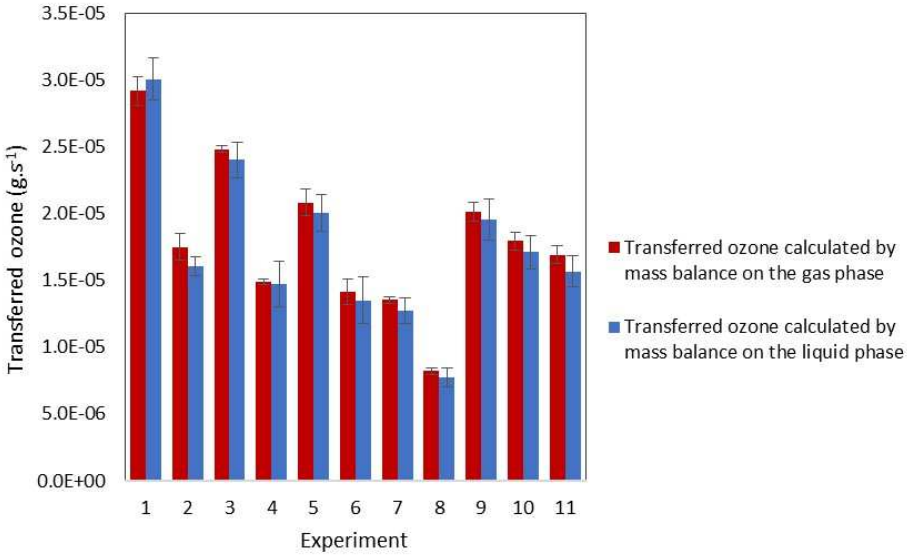

Figure 5. Transferred ozone calculated by mass balance on the gas phase vs by mass balance on the liquid phase.

(1.5-column fitting image)

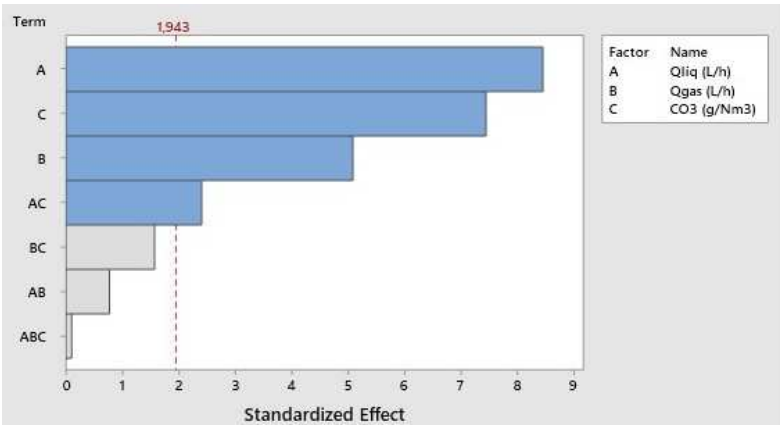

Figure 6. Pareto Chart of Standardized Effects (Response is dose of transferred ozone; α = 0.1).

(1-column fitting image, or 1.5)

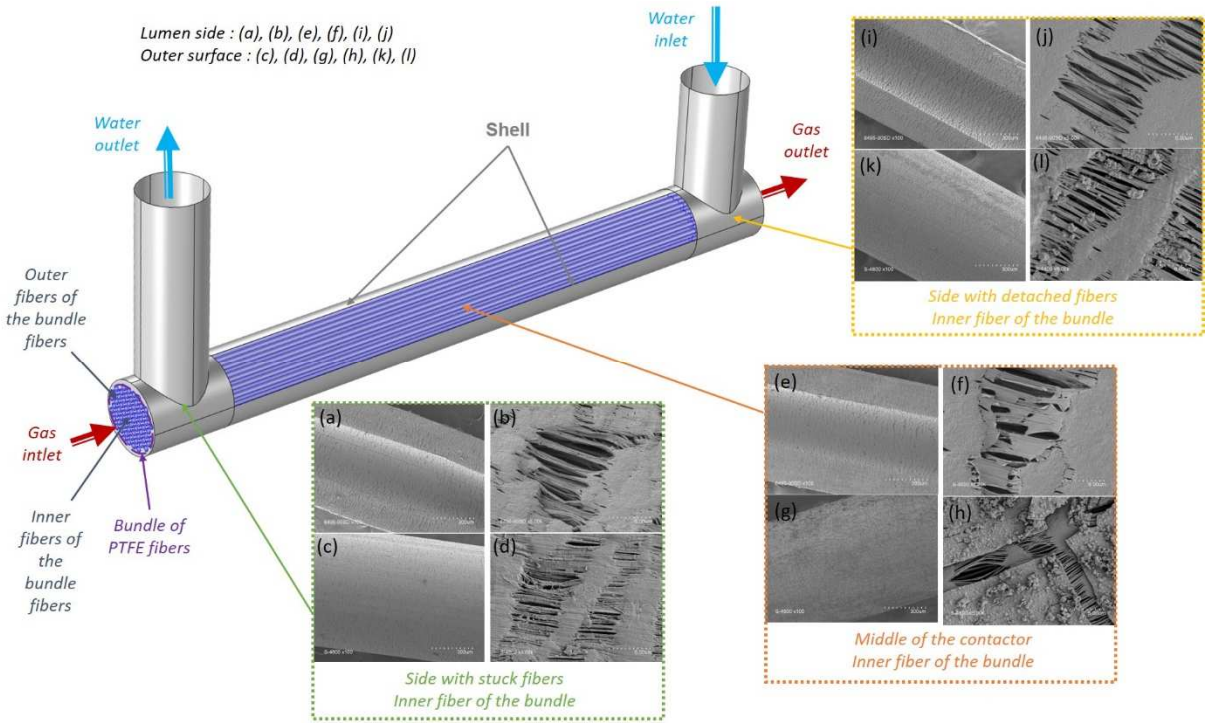

Figure 7. SEM images of an inner fiber sample of the bundle at different locations for lumen side and outer surface.

(2-column fitting image)

Tables

Suggestions of presentation are highlighted in green.

Modifications after the first submission are highlighted in yellow.

Modifications after the 2nd submission are highlighted in blue.

Table 1. Membrane contactor technical specifications.

PTFE fibers			
Number *	65	Effective length (cm) *	60
Inside diameter (mm) *	0.45	Effective outside surface (m^2)	0.107
Outside diameter (mm) *	0.87	N_2 permeance (GPU) *	33,904
Porosity [a]	0.58	Tortuosity [b]	3.47
Liquid volume (m^3) [c]	3.63×10^{-5}	Specific exchange surface a (m^2/m^3) [d]	2,948
Stainless steel shell			
Inside diameter (mm) *	9.5	Filling rate *	54.5%

** Values specified by the manufacturer (Polymem, France)*

(1-column fitting image)

Table 2. Comparison of membrane mass transfer coefficients.

Membrane material	**ε**	**τ**	**d_p (µm)**	**l_m (m)**	**$D_{O3,g}$ ($m^2.s^{-1}$)**	**D_K ($m^2.s^{-1}$)**	**$D_{O3,m}$ ($m^2.s^{-1}$)**	**k_m ($m.s^{-1}$)**	**Source**
PTFE	0.58	3.48	0.78	2.10×10^{-4}	2.00×10^{-5}	2.95×10^{-6}	2.57×10^{-6}	0.20×10^{-2}	*This study*
PTFE	0.40	6.40	0.30	1.86×10^{-4}	2.08×10^{-5}	3.64×10^{-5}	1.32×10^{-5}	0.44×10^{-2}	*Bamperng et al., 2010*
PVDF	0.75	2.08	0.20	1.75×10^{-4}	2.08×10^{-5}	2.43×10^{-5}	1.12×10^{-5}	2.31×10^{-2}	*Bamperng et al., 2010*

(2-column fitting image)

Table 3. DOE for the study of ozone transfer in buffered pure water.

Test number	Q_{liq} ($L.h^{-1}$)	Q_{gas} ($L.h^{-1}$)	C_{O3} ($g.Nm^{-3}$)
1	75	30	30
2	56.6	30	30
3	75	8	30
4	56.6	8	30
5	75	30	15
6	56.6	30	15
7	75	8	15
8	56.6	8	15
9	65.8	19	22.5
10	65.8	19	22.5
11	65.8	19	22.5

(1-column fitting image, or 1.5)

Table 4. Comparison between membrane contactor and bubble column for AO7 removal.

Reactor used	$C_{O3,gas\ inlet}$ ($g.Nm^{-3}$)	$C_{O3,gas\ outlet}$ ($g.Nm^{-3}$)	$C_{O3,liq\ outlet}$ ($mg.L^{-1}$)	$C_{AO7\ inlet}$ ($mg.L^{-1}$)	$C_{AO7\ outlet}$ ($mg.L^{-1}$)	**Applied ozone *** ($g.h^{-1}$)	**Applied ozone *** ($g.h^{-1}.{}_{treated}L^{-1}$)	**Transferred ozone **** ($g.h^{-1}$)	**Transferred ozone **** ($g.h^{-1}.{}_{treated}L^{-1}$)	**Residence time of the liquid for 34% AO7 abatement *****
Membrane contactor	30.0 (+/- 0.3)	13.0 (+/- 0.4)	0.1 (+/- 0.1)	5.2 (+/- 0.4)	3.5 (+/- 0.2)	0.240 (+/- 0.002)	6.596 (+/- 0.066)	0.136 (+/- 0.004)	3.733 (+/- 0.125)	1.7 s
Bubble column	36.9 (+/- 0.5)	*n.a.*	*n.a.*	3.9 (+/- 0.3)	*n.a.* (0 at the end of the experiment)	0.295 (+/- 0.001)	0.074 (+/- 0.001)	0.168 (+/- 0.068)	0.042 (+/- 0.017)	3.7 min (+/- 1.4)

* Calculated from the gas at the inlet
** Calculated by mass balance on the gas phase
***Initial AO7 concentration (≈ $5mg.L^{-1}$)
n.a.: Not available due to time-dependance

(2-column fitting image)

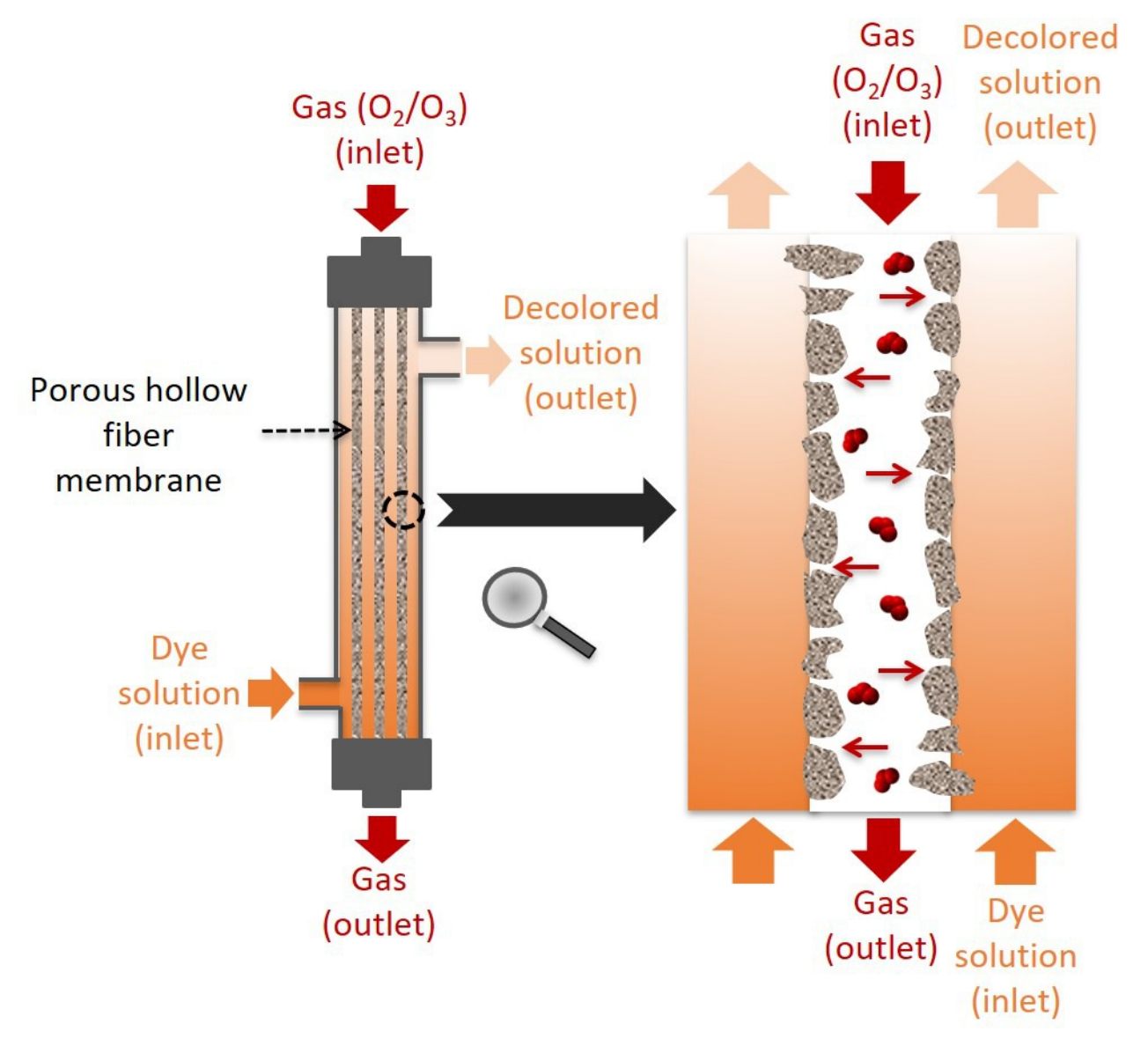
Gas (O_2/O_3) (inlet)
Decolored solution (outlet)
Porous hollow fiber membrane
Dye solution (inlet)
Gas (outlet)
Gas (O_2/O_3) (inlet)
Decolored solution (outlet)
Gas (outlet)
Dye solution (inlet)